Self-Association and Picosecond Dynamics in Liquid Dimethyl Sulfoxide

ARTICLE *in* THE JOURNAL OF PHYSICAL CHEMISTRY B · JULY 2013

Impact Factor: 3.3 · DOI: 10.1021/jp403858c · Source: PubMed

5 AUTHORS, INCLUDING:

Sviatoslav Kirillov
Joint Department of Electrochemical Energy S…
93 PUBLICATIONS **545** CITATIONS
SEE PROFILE

Kamil Rabadanov
Russian Academy of Sciences
17 PUBLICATIONS **29** CITATIONS
SEE PROFILE

THE JOURNAL OF PHYSICAL CHEMISTRY B

Article

pubs.acs.org/JPCB

Self-Association and Picosecond Dynamics in Liquid Dimethyl Sulfoxide

Sviatoslav A. Kirillov,[†,‡,*] Margarita I. Gorobets,[‡] Malik M. Gafurov,[§] Mansur B. Ataev,[§] and Kamil Sh. Rabadanov[§]

[†]Joint Department of Electrochemical Energy Systems, 38A Vernadsky Avenue, 03142 Kyiv, Ukraine

[‡]Institute for Sorption and Problems of Endoecology, 13 Gen. Naumov Street, 03164 Kyiv, Ukraine

[§]Kh. I. Amirkhanov Institute of Physics and Analytical Center of Common Access, 94 M. Yaragsky Street, 367003, Russian Federation

ABSTRACT: Dimethyl sulfoxide (DMSO) has been known for almost 150 years, but its properties as a solvent and reaction medium are far from being understood. In particular, association equilibriums in liquid DMSO have been characterized in just four papers, and the enthalpy of its self-association is unknown. The aims of this paper are to study self-association equilibriums in neat liquid DMSO at various temperatures by means of Raman spectroscopy, to find the enthalpy of self-association, and to solve the problem of hydrogen bonding in this liquid. Time correlation functions of vibrational dephasing and reorientation of coexisting monomers and dimers studied by the C−S−C and C−H symmetric vibrations indicate that external perturbations and vibrational and reorientational dynamics of these particles occur on different time scales. No signatures of H-bonding in DMSO are found. The association constants vary from 0.20 L mol^{-1} (23 °C) to 0.081 L mol^{-1} (100 °C). Their temperature dependence gives the enthalpy of association of DMSO as −11.7 ± 0.9 kJ mol^{-1}.

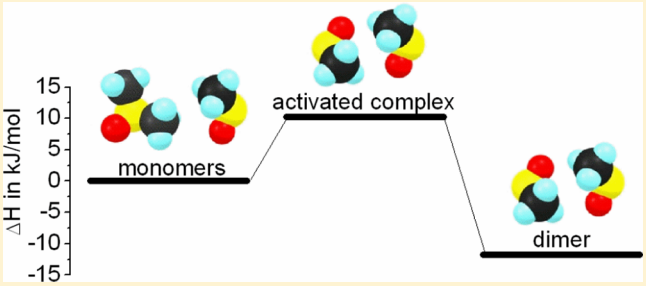

INTRODUCTION

Although dimethyl sulfoxide $(CH_3)_2SO$ (DMSO) has been synthesized 145 years ago[1] and enjoys numerous valuable applications both in industry,[2] in particular in electrochemical energy systems,[3] and in medicine,[4] the properties of this substance are far from being completely understood.[5] In the crystalline state, DMSO polymorphs stable at ambient and high pressures are described in terms of coexisting cyclic dimers formed via dipole−dipole interactions and CH···O bonded chain polymers.[6] DMSO is a highly polar liquid (dielectric constant ε = 47.24; dipole moment D = 3.96 D)[5] and as such is supposed to be self-associated and form cyclic dimers and/or linear dimers or even more complex aggregates linked by hydrogen bonds. Nevertheless, association equilibriums in liquid DMSO have been characterized in four experimental papers,[7−10] two of which were published very recently, and the enthalpy of its self-association is yet unknown.

The plethora of papers based on X-ray and neutron diffraction and molecular dynamics simulations touch upon the structure of the liquid DMSO (for a review, see ref 11); however, the formation of the cyclic dimers in the neat liquid has been convincingly proven in just a few studies.[12,13] Vibrational spectroscopic and dielectric relaxation experiments provide much more data. On the basis of the splitting of IR spectra in the region of nondegenerated S−O stretching vibration, ν_7 (A′) ∼1050 cm^{-1} (assignment according to refs 14 and 15), a conclusion has been drawn that in neat DMSO, nonassociated molecules, cyclic dimers, and chain associates are present.[16,17] The existence of the latter entities has been debated in ref 8. Furthermore, it is known that being the most intense in the infrared (IR) and having a large dipole moment derivative with respect to the vibrational normal coordinate, the ν_7 vibration of DMSO in the neat liquid and concentrated solutions is subjected to the so-called noncoincidence effect.[18−20] This phenomenon is analogous to Davydov's splitting in crystals and reflects a certain ordering in dipolar liquids.[18,21] As a result, the ν_7 line is split by several (up to four) components,[18−20] and the spectra obtained in concentrated solutions, where noncoincidences are present, cannot be interpreted unequivocally. From this point of view, measurements in the region of a less intense line corresponding to the C−S−C stretching vibration, ν_{10} (A′) ∼ 697 cm^{-1}, are considered free of possible complications.[8] As far as dielectric relaxation experiments are concerned, all of them suggest the presence of cyclic dimers in neat DMSO and its solutions.[9,10,22]

Existing data on association constants K_a obtained by means of vibrational spectroscopic methods are as follows: The first IR study dealt with the ν_7 line but in diluted CCl_4 solutions in which two components of the split line were found, and their ratio of intensities lead to K_a = 0.9 L mol^{-1}.[7] IR measurements of solutions of DMSO in acetonitrile performed in both the ν_7 and ν_{10} regions have given K_a = 0.22 L mol^{-1}.[8] Similarly, on the

Received: April 18, 2013
Revised: July 3, 2013
Published: July 18, 2013

   dx.doi.org/10.1021/jp403858c | J. Phys. Chem. B 2013, 117, 9439−9448

Table 1. Results of Data Fits and Calculations of the Parameters of the ν_{10} (A′) Line Corresponding to the C−S−C Vibrations of "Free" DMSO Molecules

t (°C)	ν^a (cm^{-1})	τ_1 (ps)	$\tau_2{}^b$ (ps)	$\delta_{is}{}^c$ (cm^{-1})	τ_v (ps)	τ_ω (ps)	M_2 (ps^{-2})
			isotropic				
30	664.3	0.08 ± 0.02	0.718	15.4	0.79 ± 0.02	0.08 ± 0.02	17 ± 4
40	663.9	0.06 ± 0.01	0.708	14.9	0.76 ± 0.01	0.06 ± 0.01	4 ± 2
50	663.5	0.07 ± 0.01	0.695	15.6	0.76 ± 0.01	0.07 ± 0.01	22 ± 5
60	663.8	0.20 ± 0.02	0.672	15.2	0.83 ± 0.02	0.21 ± 0.02	7 ± 2
70	663.2	0.12 ± 0.02	0.674	15.2	0.77 ± 0.02	0.12 ± 0.02	13 ± 3
80	663.1	0.12 ± 0.01	0.665	15.4	0.77 ± 0.02	0.13 ± 0.02	12 ± 3
90	662.9	0.21 ± 0.02	0.642	15.5	0.80 ± 0.02	0.23 ± 0.02	7 ± 2
100	662.7	0.18 ± 0.01	0.641	15.9	0.78 ± 0.01	0.18 ± 0.01	9 ± 2

t (°C)	ν^a (cm^{-1})	τ_1 (ps)	τ_2 (ps)	$\delta_{anis}{}^c$ (cm^{-1})	M_{2anis} (ps^{-2})	$\delta_{2R}{}^d$ (cm^{-1})	τ_{2R} (ps)	M_{2R} (ps^{-2})	$I \times 10^{40}$ (g cm^2)
			anisotropic				rotational		
30	664.6	0.04 ± 0.01	0.60 ± 0.05	17.5	48 ± 9	2.1	3.4 ± 0.8	31 ± 11	81 ± 29
40	663.5	0.04 ± 0.01	0.60 ± 0.05	17.7	46 ± 9	2.8	3.7 ± 0.8	23 ± 11	113 ± 54
50	664.1	0.04 ± 0.01	0.58 ± 0.04	18.5	49 ± 9	2.9	3.2 ± 0.8	27 ± 14	99 ± 51
60	663.8	0.04 ± 0.01	0.53 ± 0.06	19.3	53 ± 10	4.1	2.1 ± 0.4	50 ± 12	55 ± 13
70	663.8	0.03 ± 0.01	0.53 ± 0.06	19.8	60 ± 10	4.6	2.3 ± 0.5	47 ± 13	60 ± 17
80	663.9	0.03 ± 0.01	0.53 ± 0.06	19.8	61 ± 10	4.4	2.4 ± 0.5	49 ± 13	59 ± 17
90	663.8	0.04 ± 0.01	0.49 ± 0.07	21.3	55 ± 10	5.8	1.7 ± 0.4	39 ± 12	77 ± 24
100	663.6	0.03 ± 0.01	0.49 ± 0.07	21.5	71 ± 12	5.6	1.7 ± 0.4	62 ± 14	49 ± 11

[a]Less than 0.03 cm^{-1} uncertainty. [b]Less than 1% uncertainty. [c]±0.05 cm^{-1} uncertainty. [d]±0.1 cm^{-1} uncertainty.

basis of IR and Raman investigations in the ν_{10} region supplemented with dielectric relaxation studies of solutions of DMSO in CCl_4 or benzene, K_a values for diluted solutions were found to be 2.5 or 0.7 L mol^{-1}, respectively, whereas in concentrated solutions and neat DMSO, they are close to 20−40 L mol^{-1}.[9] In a preceding paper, the same authors claim that for neat DMSO dielectric measurements give K_a = 60 L mol^{-1}.[10]

The presence of association equilibriums in DMSO should significantly complicate its picosecond dynamics. Collisions and vibrational and reorientational processes involving monomer and dimer molecules should occur on different time scales. However, information regarding picosecond dynamics in neat DMSO is scarce.[23,24] Such data, obtainable in vibrational spectroscopic experiments,[25,26] can be of great help for better understanding the nature of association phenomena.

As far as hydrogen bonding is concerned, distinct spectroscopic signatures of this phenomenon have not been found in neat DMSO. However, the possible presence of H-bonds is discussed for higher sulfoxides.[27] Although in early molecular dynamics simulations hydrogen atoms of methyl groups were considered to be involved in H-bonding, more detailed studies[28] suggested that sharp peaks on C−O radial distribution functions are not necessarily the signature of H-bonds between DMSO molecules.

The aims of this paper are to study self-association equilibriums in neat liquid DMSO at various temperatures by means of Raman spectroscopy, to find the enthalpy of self-association, and to solve the problem of hydrogen bonding in this liquid. In order to distinguish between dimers, monomers, and H-bonded molecules, we explicitly employ, for the first time, the notion of vibrational and rotational dynamics of molecular liquids.[25,26]

EXPERIMENTAL SECTION

DMSO (Sigma-Aldrich 276855, ≥99.9%, melting temperature 18.5 °C) was used as received. It was flame-sealed in a 5 mm inner diameter Pyrex tube. Raman spectra were excited by the 532 nm line of a solid state Nd:YAG laser and registered on a confocal Raman microscope (Senterra, Bruker, Germany) with a 20× camera lens, a 50 × 100 mkm slit, and a resolution of 3−5 cm^{-1}. At least 20 scans were accumulated at polarized (I_{VV}) and depolarized (I_{VH}) scattering geometries with the integration time of 20 s. The first and the second letters in subscripts denote the state of polarization of the incident and scattered radiation, respectively; V stands for vertical and H for horizontal. Knowing I_{VV} and I_{VH}, the isotropic and anisotropic line profiles were calculated as

$$I_{iso}(\nu) = I_{VV}(\nu) - \frac{4}{3} I_{VH}(\nu) \quad (1)$$

$$I_{aniso}(\nu) = I_{VH}(\nu) \quad (2)$$

Raman spectra were collected in the temperature range of 23−100 °C. For high-temperature studies, a special heating device placed on the microscope stage was designed enabling one to heat the sample to 140−150 °C. The presence of a heat shield and the constant blowing of air on the lens minimize the effect of heating on the sensitive optics of the instrument. The temperature was controlled with an uncertainty of 0.5 K. Before each measurement, the temperature was stabilized for at least 0.5 h. Registrations were made on stepwise heating, and control runs on cooling showed excellent reproducibility of the spectra with fitting uncertainties falling within the ranges given in Tables 1−3.

Intending to analyze the signatures of dimerization, we operate with the polarized Raman line at approximately 670 cm^{-1}, corresponding to the ν_{10} (A′) vibration (symmetric C−S−C stretching mode), which is sensitive to the association equilibrium. For studying H-bonding phenomena, we monitor the polarized Raman line at approximately 2910 cm^{-1}, corresponding to the ν_3 (A′) vibration (the symmetric C−H stretching mode). In these same regions, other depolarized Raman lines are also visible corresponding to the asymmetric

dx.doi.org/10.1021/jp403858c | J. Phys. Chem. B 2013, 117, 9439−9448

Table 2. Results of Data Fits and Calculations of the Parameters of the ν_{10} (A′) Line Corresponding to the C−S−C Vibrations of Bonded DMSO Molecules

t (°C)	ν^a (cm^{-1})	$\tau_1{}^b$ (ps)	$\tau_2{}^b$ (ps)	$\delta_{is}{}^c$ (cm^{-1})	$\tau_v{}^b$ (ps)	$\tau_\omega{}^b$ (ps)	$M_2{}^d$ (ps^{-2})
				isotropic			
30	668.8	1.78	0.722	8.7	1.62	2.60	0.78
40	668.5	1.73	0.729	9.1	1.61	2.46	0.80
50	668.0	1.82	0.707	9.3	1.61	2.70	0.78
60	668.0	2.03	0.697	8.5	1.66	2.99	0.72
70	667.5	2.19	0.659	9.0	1.66	3.50	0.69
80	667.5	2.12	0.668	8.9	1.65	3.36	0.71
90	667.1	2.17	0.671	8.8	1.67	3.37	0.69
100	667.0	2.15	0.660	9.0	1.65	3.42	0.71
t (°C)	ν^a (cm^{-1})	τ_1 (ps)	τ_2 (ps)	$\delta_{anis}{}^c$ (cm^{-1})	M_{2anis} (ps^{-2})		
				anisotropic			
30	668.7	3.3 ± 0.3	0.44 ± 0.03	9.8	0.69 ± 0.06		
40	668.6	3.0 ± 0.3	0.51 ± 0.04	9.3	0.66 ± 0.06		
50	668.1	3.3 ± 0.3	0.47 ± 0.04	9.3	0.64 ± 0.06		
60	667.6	3.3 ± 0.3	0.43 ± 0.04	9.9	0.71 ± 0.07		
70	667.6	3.4 ± 0.3	0.46 ± 0.04	9.3	0.64 ± 0.07		
80	667.7	3.6 ± 0.4	0.48 ± 0.04	8.7	0.58 ± 0.08		
90	667.1	3.3 ± 0.4	0.48 ± 0.04	9.2	0.65 ± 0.08		
100	667.1	3.5 ± 0.4	0.46 ± 0.04	9.2	0.62 ± 0.08		

[a]Less than 0.03 cm^{-1} uncertainty. [b]Less than 1% uncertainty. [c]±0.05 cm^{-1} uncertainty. [d]±0.02 ps^{-2} uncertainty.

C−S−C stretching mode, ν_{28} (A″), at approximately 700 cm^{-1}, and the C−H stretching mode, ν_{14} (A″), at approximately 3000 cm^{-1}. Though their split profiles have been taken into account in data fits (see below), their behavior is not considered in this paper because of the depolarized nature of these lines and hence the inseparability of the contributions of vibrational and rotational dynamics to the profiles.[25,26] In order to monitor the degree of polarization of respective lines, the wavenumber dependences of the depolarization ratio, $\rho = I_{VV}/I_{HV}$, have been calculated.

In measurements of concentrations using Raman data, integrated intensities of Raman lines were considered proportional to concentrations,[29,30] and no corrections for possible differences in the scattering abilities of monomers and dimers were introduced. This is justified by the data published by several authors who claim small concentration dependences of the scattering abilities of free and solvating DMSO molecules in ionic solutions.[31,32]

THEORETICAL BACKGROUND AND COMPUTATION DETAILS

Studies of vibrational and rotational relaxation of probe molecules in liquids by means of spontaneous Raman spectroscopy employ the apparatus of time-correlation functions (TCFs) $G_V(t)$ and $G_{2R}(t)$, obtainable by means of Fourier transformation of isotropic and anisotropic Raman spectra $I_{iso}(\nu)$ and $I_{aniso}(\nu)$, respectively,[21,25,26]

$$G_V(t) = \int_{-\infty}^{+\infty} I_{iso}(\nu) \exp(2\pi i c\nu t)\, d\nu \quad (3)$$

$$G_{2R}(t) = \int_{-\infty}^{+\infty} I_{aniso}(\nu) \exp(2\pi i c\nu t)\, d\nu / G_V(t) \quad (4)$$

where c is the speed of light and ν is the frequency measured in wavenumbers. The subscript 2 in $G_{2R}(t)$ means that in Raman rotation is represented by the spherical harmonics of the second order.

Quite often, isotropic line broadening is considered in terms of the so-called vibrational dephasing caused by adiabatic

Table 3. Results of Data Fits and Calculations of the Parameters of the ν_3 (A′) Line Corresponding to the C−H Vibrations of DMSO Molecules

t (°C)	ν^a (cm^{-1})	$\tau_1{}^b$ (ps)	$\tau_2{}^c$ (ps)	$\delta_{is}{}^d$ (cm^{-1})	$\tau_v{}^c$ (ps)	$\tau_\omega{}^b$ (ps)	$M_2{}^e$ (ps^{-2})
				isotropic			
23	2913.0	0.406	0.875	11.0	1.18	0.430	2.82
30	2913.5	0.384	0.898	10.8	1.19	0.405	2.90
40	2913.3	0.367	0.908	10.8	1.19	0.385	3.00
50	2913.5	0.355	0.919	10.7	1.19	0.372	3.06
60	2913.5	0.346	0.927	10.7	1.19	0.361	3.12
70	2913.5	0.345	0.932	10.6	1.20	0.360	3.12
80	2913.6	0.344	0.936	10.6	1.20	0.359	3.11
90	2913.7	0.344	0.940	10.5	1.20	0.359	3.09
100	2913.7	0.344	0.940	10.5	1.20	0.359	3.09
t (°C)	ν^a (cm^{-1})	τ_1 (ps)	$\tau_2{}^f$ (ps)	$\delta_{anis}{}^d$ (cm^{-1})	M_{2anis} (ps^{-2})	δ_{2R} (cm^{-1})	$\tau_{2R}{}^g$ (ps)	M_{2R} (ps^{-2})
				anisotropic			rotational	
23	2913.7	0.015 ± 0.005	0.95	11.3	70 ± 25	0.3	35	67 ± 25
30	2913.8	0.015 ± 0.005	0.92	11.6	74 ± 25	0.8	14	71 ± 25
40	2913.8	0.015 ± 0.005	0.91	11.7	75 ± 25	0.9	12	72 ± 25
50	2913.9	0.017 ± 0.006	0.91	11.8	70 ± 24	1.1	10	64 ± 24
60	2913.9	0.020 ± 0.007	0.92	11.7	54 ± 15	1.0	10	51 ± 15
70	2913.7	0.021 ± 0.007	0.90	11.8	53 ± 15	1.2	9	50 ± 15
80	2914.0	0.023 ± 0.008	0.92	11.5	47 ± 15	1.1	11	44 ± 15
90	2914.0	0.066 ± 0.015	0.92	11.5	16 ± 8	1.0	10	13 ± 8
100	2914.0	0.031 ± 0.010	0.92	11.5	35 ± 16	1.0	10	32 ± 16

[a]Less than 0.03 cm^{-1} uncertainty. [b]Less than 2% uncertainty. [c]Less than 1% uncertainty. [d]±0.05 cm^{-1} uncertainty. [e]±0.02 ps^{-2} uncertainty. [f]±0.02 ps uncertainty. [g]$\tau_{2R} = (\pi c \delta_{2R})^{-1}$.

dx.doi.org/10.1021/jp403858c | J. Phys. Chem. B 2013, 117, 9439−9448

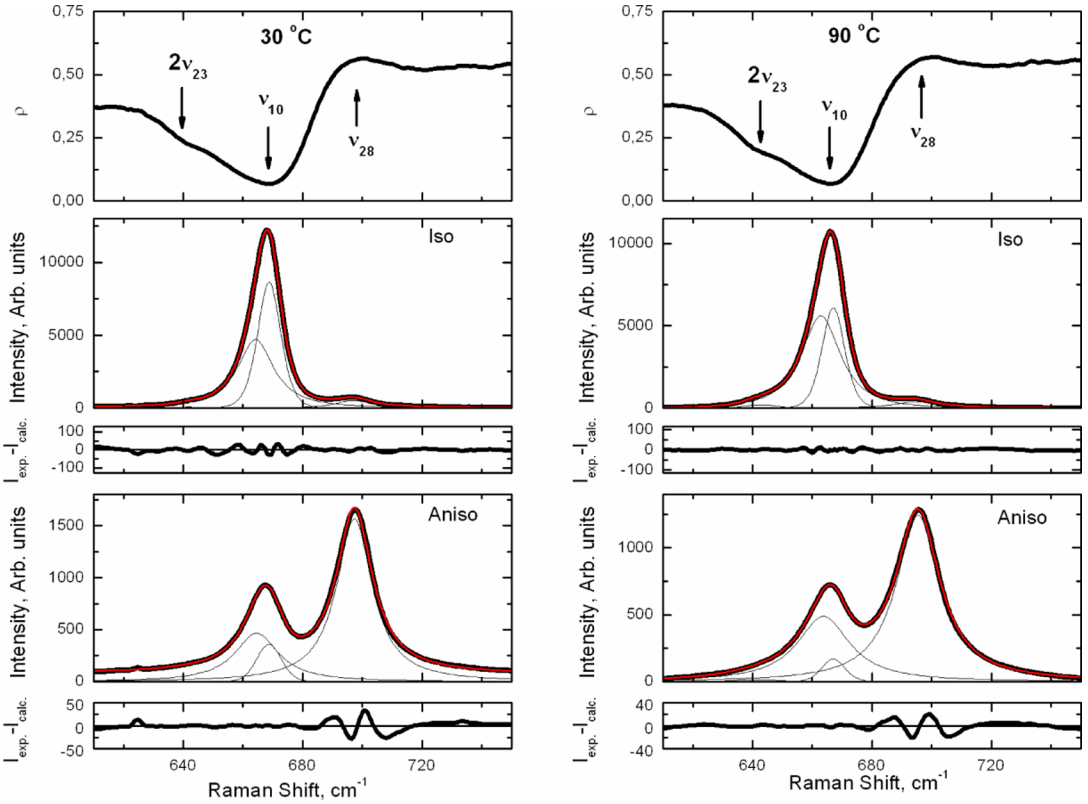

Figure 1. Temperature evolution of Raman spectra of dimethyl sulfoxide in the region of the ν_{10} (A′) and ν_{22} (A″) vibrations. Left panel, 30 °C; right panel, 90 °C. $I_{exp} - I_{calc}$ scales are 1% and 3% of the peak intensities of the most intense isotropic and anisotropic lines, respectively.

perturbations of the probe molecule by its surroundings. These perturbations modulate molecular vibrations and give rise to phase shifts. The TCF of vibrational dephasing is written by the Kubo equation[33]

$$G_V(t) = M_2\tau_\omega^2 e^{-\exp(-t/\tau_\omega)-1+t/\tau_\omega} \quad (5)$$

where τ_ω is the modulation (perturbation) time and $M_2 = \int \nu^2 I_{iso}(\nu)\, d\nu / \int I_{iso}(\nu)\, d\nu$ is the isotropic (vibrational) second moment (perturbation dispersion).

Depending on the perturbation time, TCFs and spectra are changing. If $\tau_\omega \rightarrow 0$ (perturbations are weak and fast, interactions are nonspecific, and the surroundings of the probe particle are flexible), the TCFs are exponential and the spectra are of the Lorentzian form. In this case, it is quite common to describe modulation phenomena in terms of collision concepts and to consider modulation to be collision driven. If $\tau_\omega \rightarrow \infty$ (perturbations are strong and slow, interactions are specific and directed, and the particle and its surroundings form a rigid quasilattice), the TCFs and the spectra become Gaussian. On the basis of these considerations, one may describe modulation processes in terms of collision concepts by attributing τ_ω as the time between collisions τ_{BC} of the probe particle with neighboring particles. Another characteristic of the process is the dephasing time τ_V determined as the integral of $G_V(t)$, $\tau_V = \int G_V(t)\, dt$.

As far as rotational TCFs are concerned, these can be described by an equation similar to eq 5 with the characteristic time having the meaning of the correlation time of the angular momentum τ_J

$$G_{2R}(t) = M_{2R}\tau_J^2 e^{-\exp(-t/\tau_J)-1+t/\tau_J} \quad (6)$$

$M_{2R} = \int \nu^2 I_{aniso}(\nu)\, d\nu / \int I_{aniso}(\nu)\, d\nu - M_2$ is the anisotropic or rotational second moment, and $\tau_{2R} = \int G_{2R}(t)\, dt$.

In spite of the fact that time-dependent interactions are now extensively explored with sophisticated pico- and femtosecond spectroscopic methods,[34] approaches based on simple line profile analyses remain in use in studies of condensed media, including ionic and molecular liquids, glasses, and polymers.[35−39]

In order to perform the decomposition of overlap Raman spectra and to compute TCFs, a method described in ref 40 was utilized. It is based on a model TCF

$$G_v(t) = \exp\{-[(t^2 + \tau_1^2)^{1/2} - \tau_1]/\tau_2\} \quad (7)$$

where τ_1 and τ_2 are certain times related to the dephasing time as $\tau_V = (\tau_2^2 + 2\tau_1\tau_2)^{1/2}$. This TCF perfectly matches the Kubo function (eq 5). Moreover, its Fourier transform can be performed analytically giving the following expression for the line profile:

$$I(V) = 2nc \exp(\tau_1/\tau_2)(\tau_1^2/\tau_2)K_1(x)/x \quad (8)$$

where $x = \tau_1[4\pi^2c^2(\nu - \nu_0)^2 + 1/\tau_2^2]^{1/2}$ and ν_0 is the wavenumber of the peak frequency of the line; $n = 2$ at $\nu_0 = 0$ and $n = 1$ at $\nu_0 \neq 0$. $K_1(x)$ is the modified Bessel function of the second kind. This method has been widely employed for the treatment of spectroscopic data,[21,41] especially in cases of overlapping lines. The algorithm of its use is described in detail in refs 21 and 41.

RESULTS AND DISCUSSION

Preliminary Remarks. On the basis of considerations presented in previous sections, one can expect the following

dx.doi.org/10.1021/jp403858c | J. Phys. Chem. B 2013, 117, 9439−9448

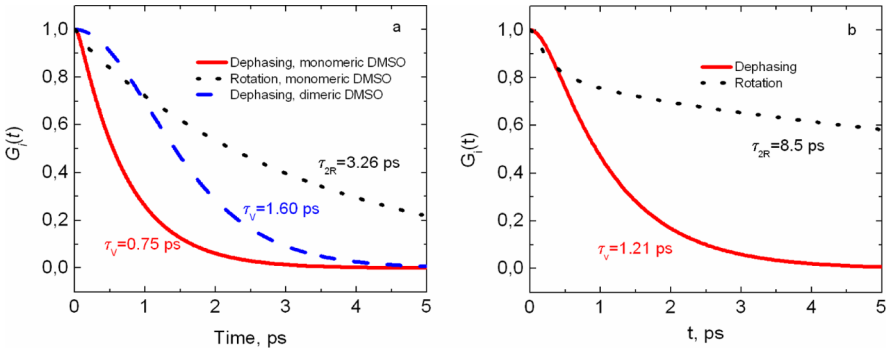

Figure 2. Representative time-correlation functions of dephasing and reorientation of dimethyl sulfoxide molecules determined from the components of the lines corresponding to (a) the ν_{10} (A′) vibrations of monomeric and dimeric DMSO molecules at 50 °C and (b) the lines corresponding to the ν_3 (A′) vibrations of DMSO molecules at 90 °C.

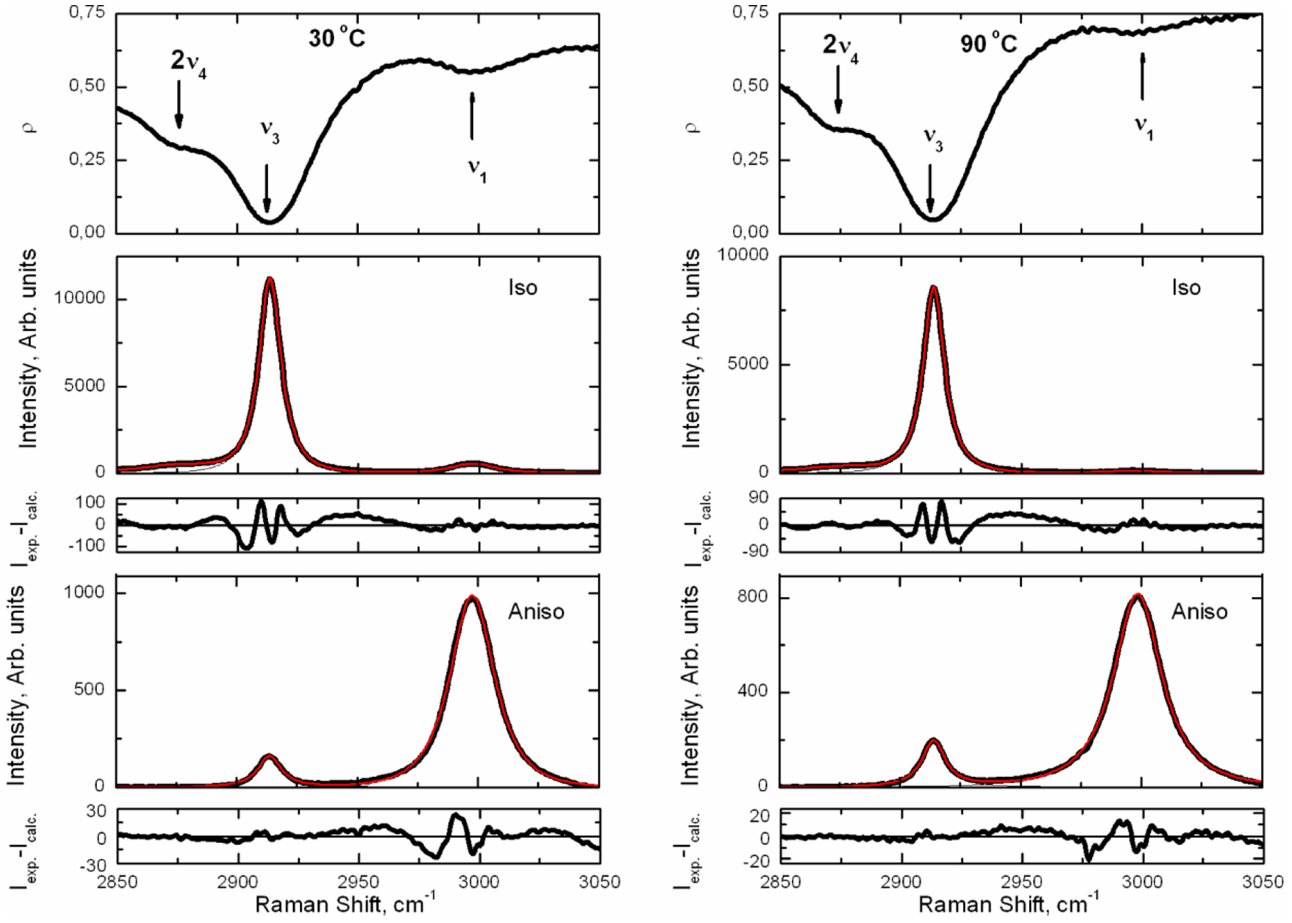

Figure 3. Temperature evolution of Raman spectra of dimethyl sulfoxide in the region of the ν_3 (A′) and ν_{14} (A″) vibrations. Left panel, 30 °C; right panel, 90 °C. $I_{exp} - I_{calc}$ scales are 1% and 3% of the peak intensities of the most intense isotropic and anisotropic lines, respectively.

behavior of vibrational lines corresponding to monomeric and dimeric DMSO molecules: The surroundings of the monomers are flexible and moveable, and vibrational frequency modulation can be described using fast perturbation concepts. Monomeric molecules have no significant difficulties in executing their rotations. On the contrary, neighboring molecules in dimers are tightly bond together, and vibrational frequency modulation should reflect the slow perturbation limit. Rotational motion of heavy, bulky dimers should be frozen or, at least, much slower than that of monomers. From this point of view, the shape of the isotropic (and anisotropic) lines corresponding to the symmetric C−S−C stretching mode in monomers should be more Lorentzian than that of dimers. Because of slow reorientation of dimers and hence small reorientational contributions to the anisotropic line profile, respective isotropic and anisotropic lines should be of similar width.

Similar considerations should be addressed in analyses of the lines corresponding to the symmetric C−H stretching vibrations of "free" and H-bonded molecules in dimers and monomers.

In practice, these expectations look less optimistic. We deal with similar probe oscillators belonging to different particles, that is, monomers and dimers existing in different environ-

dx.doi.org/10.1021/jp403858c | J. Phys. Chem. B 2013, 117, 9439−9448

ments, involved in different interactions, experiencing unequal perturbations, and executing different elementary motions (rotations). Unlike in the vast majority of analogous studies of dynamics, the mentioned perturbations in our case are of commensurable magnitudes, and vibrational frequencies of the probe oscillators in monomers and dimers can be almost the same, giving superposed, indivisible vibrational lines.

Vibrational Relaxation of DMSO Molecules. In the whole temperature range studied, ordering in DMSO is clearly seen in vibrational spectra in the region corresponding to the symmetric C−S−C stretching mode, where the isotropic and anisotropic lines are split into two components at ∼663 and ∼668 cm^{-1} (Figure 1). Data fits (Tables 1 and 2) reveal that in isotropic spectra the low-frequency component is more Lorentzian in shape and the high-frequency component is more Gaussian. Their respective vibrational TCFs are different. For example, at 30 °C (Figure 2a), the low-frequency component having a more exponential TCF relaxes quickly (τ_V = 0.76 ps), and its modulation time τ_ω equals 0.07 ps. The high-frequency component has a more Gaussian TCF. It relaxes more slowly (τ_V = 1.61 ps), and its modulation time (τ_ω = 2.70 ps) is 30 times greater than that of the low-frequency component. Such differences signify that the low-frequency component corresponds to free (monomeric) DMSO molecules whose vibrations are modulated by a fast process, whereas the high-frequency component corresponds to dimeric DMSO molecules rigidly connected together by specific interactions influencing the C−S−C oscillator.

Unlike the lines corresponding to the C−S−C stretching modes, the polarized Raman line at approximately 2910 cm^{-1} corresponding to the ν_3 (A′) vibration, the symmetric C−H stretching mode, demonstrates no splitting, suggesting that hydrogen bonding is not the cause of ordering in the liquid (Figure 3 and Table 3). The absence of splitting means that perturbations influencing C−H bonds in monomers and dimers are of similar magnitude. These bonds are indiscernible in Raman because vibrations corresponding to them are of the same frequency. The respective TCFs (Figure 2a) exhibit relaxation slower than those of the C−S−C stretching (τ_V ∼ 1.2 ps), and their modulation times τ_ω values equal 0.36−0.43 ps, signifying fast modulation of the C−H stretching vibration in accord with existing Raman data.[21,22] However, these τ_ω are 1 order of magnitude greater than those of the C−S−C stretching in monomeric DMSO molecules; such a phenomenon requires commenting.

To discern between possible mechanisms causing vibrational frequency modulation, we have attempted to find its motive force. In dephasing studies, as mentioned above, it is customary to treat τ_ω in terms of binary collisions: $\tau_\omega \approx \tau_{BC}$.[33] To estimate the τ_{BC} value, the Enskog model[42] is the most common, despite its shortcomings mentioned in ref 43. It predicts the dependence of τ_{BC} on the collision diameter σ and the reduced mass m of colliding particles as

$$\tau_{BC} = [4\sigma^2 N\, g(\sigma)]^{-1}[2m/(\pi k_B T)]^{1/2} \quad (9)$$

where $N = N_A/V_M$ is the number density of the system (N_A is Avogadro's number and V_M is the molar volume), $g(\sigma)$ the radial distribution function which may be considered equal to unity,[42] k_B the Boltzmann constant, and T the temperature.

Using the density of DMSO,[44] one approximates σ = 4.9 Å and gets τ_{BC} = 0.39 ps; its temperature dependence is negligible. If the collision diameter and the reduced mass are increased and the number density of the system is decreased so as to model collisions in the system containing dimers, τ_{BC} values decrease by not more that 50%. This means that in the case of the symmetric C−H stretching mode having τ_ω = 0.36−0.43 ps, the modulation time and τ_{BC} perfectly coincide. Regardless of the nature of colliding particles (either monomers or dimers), the modulation process can be considered in terms of binary collisions.

For the symmetric C−S−C stretching mode in DMSO monomers, the modulation process is faster than τ_{BC} (Table 1). In order to find its motive force, we recall that the phase shifts are known to be caused by various perturbations, including (from slow to fast) structure relaxation, reorientations, vibrational relaxation, binary collisions, and large amplitude vibrational motion of the probe (or attached) oscillator with wavenumbers ν less than ∼250 cm^{-1}.[45] The sequence of respective characteristic times is $\tau_S \geq \tau_{IR} \approx \tau_V \geq \tau_{BC} > \tau_{vibr}$, where τ_{vibr} is the half-period of vibration, $\tau_{vibr} = 1/2c\nu$. In this sequence, we omit nonadiabatic processes reviewed in ref 46; it should be also noted that, considering modulation rates in liquids, one should account for the presence of a probability factor $\kappa \leq 1$ determining the ability of i-th modulation attempts to produce a phase shift, $\tau_\omega^{-1} = \kappa\tau_i^{-1}$.[47]

Among prospective candidates influencing the C−S−C oscillator in monomers are torsional vibrations of the attached CH_3 groups. Although internal rotations of the methyls in DMSO meet a high potential barrier (∼17.2 kJ mol^{-1})[48] and are hindered, their torsions (ν_{tors} = 219 cm^{-1} in ref 14 or ν_{13} (A′) = 159 cm^{-1} and ν_{24} (A″) = 152 cm^{-1} in ref 15) can perturb the C−S bonds because of large vibrational amplitudes of the light hydrogen atoms. Using $\nu \approx$ 155−219 cm^{-1} for these vibrations, we get τ_{vibr} = 0.11−0.076 ps. That is close to τ_ω = 0.06−0.23 ps (Table 1).

Reorientation of DMSO Molecules. The TCFs of reorientations of DMSO molecules determined from the low-frequency line at ∼670 cm^{-1} reflect molecular rotations occurring each τ_{2R} = 1.7−3.7 ps (Figure 2, Table 1) and evidence the monomeric nature of rotating entities. Such τ_{2R} values are in a good agreement with the data obtained by dielectric relaxation spectroscopy,[8,9] τ_{1R} = 4.5−5.0 ps. As expected, τ_{1R} is greater than τ_{2R} because dielectric relaxation experiments measure vector properties (the subscript 1 means the spherical harmonics of the first order), whereas Raman spectroscopy measures tensor properties, and $\tau_{1R}/\tau_{2R} \approx 1.5$.[7,8] It should be mentioned that TCFs simulated in molecular dynamics studies (see ref 10 and references therein) reveal quite long characteristic times compared to experimentally measured values.

Rotations of "bonded" DMSO molecules characterized by means of dielectric relaxation are much slower,[8,9] τ_{1R} = 19−23 ps. Such times are indiscernible in Raman experiments, resulting in $G_{2R}(t)$ = 1 in the picosecond time domain (not shown in Figure 2a) and in coinciding isotropic and anisotropic line profiles (Table 2). It is worth mentioning that in Rayleigh experiments sensitive to collective properties[25,26] (unlike Raman experiments which are sensitive to single-particle properties[25,26]), mean reorientation times τ_{2R} in liquid DMSO at 22−70 °C fall within 8.6−3.4 ps,[49] lying just between the values obtained for the monomers and dimers.

For the monomeric DMSO molecules, considerations regarding fast processes influencing vibrational dephasing are well-supported by the analysis of reorientational dynamics. In the theory of rotational relaxation presented by Gordon,[50] the

dx.doi.org/10.1021/jp403858c | J. Phys. Chem. B 2013, 117, 9439−9448

second rotational moment $M_{2R}(2)$ is determined by the moment of inertia of the molecule I

$$M_{2R}(2) = 6k_BT/I \quad (10)$$

The DMSO molecule belongs to a low-symmetry point group (C_s) and has three different moments of inertia[12] equal to 119.3, 121.5, and 199.1 × 10^{-40} g cm^2. For asymmetric tops, it is impossible to apply "selection rules" for reorientation[47] and to distinguish between rotation processes occurring around different molecular axes; one can rather describe a generalized reorientation involving all axes with the mean geometrical value of I = 142.4 × 10^{-40} g cm^2. Calculations based on experimental data (Table 1) give I = 49−113 × 10^{-40} g cm^2. Even though they are determined with a great uncertainty, they never exceed the minimal value of the moment of inertia of DMSO and do not contradict the idea of single-molecule reorientations.

Additional information about intimate details of the reorientation process of the monomeric molecules follows from the analysis of the small-time behavior of the TCF of reorientations. Theoretically,[50−52] Raman scattering probes correlations between tensors that are predicted to vanish if the angle between their main axes reaches 41°. Such a rotation may be performed in one step, as in the case of free rotation or great-angle jumps, or may consist of many uncorrelated small-angle elementary angular steps φ_{FR}, where at each step a molecule moves as a free rotor during the time τ_{FR}. τ_{FR} and φ_{FR} are connected by the following equation:[50]

$$\tau_{FR} = \frac{\varphi_{FR}}{360^\circ} 2\pi \left(\frac{I_i}{k_BT}\right)^{1/2} \quad (11)$$

Experimentally, φ_{FR} and τ_{FR} can be found by means of a comparison of $G_{2R}(t)$ with the TCF for a classical ensemble of freely rotating molecules[50,53]

$$G_{2R}^{FR}(t) = \exp\left(-\frac{3k_BT}{I_i}t^2\right) = \exp\left[-\frac{M_{2R}(2)}{2}t^2\right] \quad (12)$$

The time at which $G_{2R}^{FR}(t)$ and $G_{2R}(t)$ diverge provides an estimate of the maximal time of free rotation. These correlation functions are shown in Figure 4, where two approximations are considered at 30 °C. For the calculated $M_{2R}(2)$ = 17.6 ps^{-2} (I = 142.4 × 10^{-40} g cm^2), the free rotation time is τ_{FR} = 0.072 ps, whereas for the experimental $M_{2R}(2)$ = 31 ps^{-2} (I = 81 × 10^{-40} g cm^2), free rotations occur with τ_{FR} = 0.045 ps. Using eq 11, this yields φ_{FR} = 5.9−7.1°. On the one hand, knowing τ_{2R} = 3.26 ps, one concludes that each reorientation by 41° consists of τ_{2R}/τ_{FR} = 45−75 elementary steps and the reorientation of single DMSO molecules could be considered as free medium-angle diffusion.[54] On the other hand, these τ_{FR} values are quite close to $\tau_\omega \approx \tau_{vibr}$ = 0.11−0.076 ps and support our conjecture regarding the role of the CH_3 torsions in the modulation events.

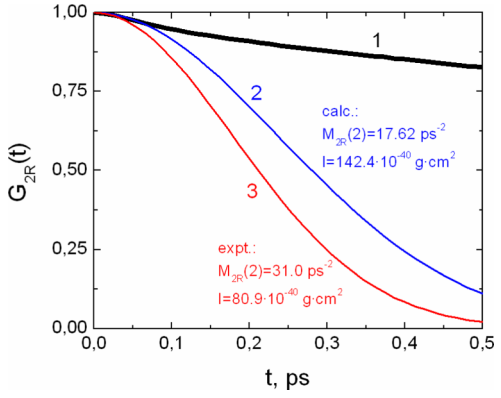

Figure 4. Small-time behavior of the time-correlation functions of reorientation of monomeric molecules of dimethyl sulfoxide at 30 °C. Black line (1), $G_{2R}(t)$; blue line (2), $G_{2R}^{FR}(t)$ with $M_{2R}(2)$ = 18 ps^{-2}; and red line (3), $G_{2R}^{FR}(t)$ with $M_{2R}(2)$ = 31 ps^{-2}.

Reorientation times of DMSO molecules determined either from the lines corresponding to the C−H vibrations as $\tau_{2R} = [\pi c(\delta_{anis} - \delta_{is})]^{-1}$, where δ_{anis} and δ_{is} are the widths of anisotropic and isotropic lines, respectively (Table 3), or from TCFs (Figure 2b) are in the range of 9−15 ps. This is probably due to the inability to discern between monomers and dimers in this spectral region. Such complications do not significantly influence the isotropic lines, where dephasing and modulation times for monomers and dimers are commensurable. However, in the case of the reorientational portions of the anisotropic lines, the slow contributions caused by dimers prevail.

Self-Association Equilibrium. Before we characterize the self-association equilibrium in the liquid DMSO, let us summarize differences in the vibrational manifestations of monomeric and dimeric molecules. The hierarchy of characteristic times for the symmetric C−S−C vibrational mode, which manifests itself at ∼663 cm^{-1}, $\tau_{2R} > \tau_V > \tau_{BC} \gg \tau_\omega$ ($\approx \tau_{vibr} \approx \tau_{FR}$), clearly signifies that this mode belongs to the monomeric molecule. The hierarchy for the mode showing up at ∼668 cm^{-1}, $\tau_{2R} > \tau_\omega \gg \tau_V > \tau_{BC}$, is peculiar for the dimeric molecules. This justifies the use of the respective lines in the calculations of equilibrium constants. In reality, the intensity of the low-frequency line at ∼670 cm^{-1} grows on heating, and that of the high-frequency line at ∼668 cm^{-1} decreases. This fact implies the decomposition of dimers. On the other hand, the symmetric CH_3 vibrational mode with the hierarchy of characteristic times $\tau_{2R} > \tau_V > \tau_\omega$ ($\approx \tau_{BC}$) does not perceive the presence of monomers and/or dimers, manifesting itself as a single line at 2910 cm^{-1} that cannot be used in equilibrium studies.

Expressing an equilibrium between the dimeric and monomeric molecules as

$$2\text{DMSO} = (\text{DMSO})_2 \quad (13)$$

one can write the association constant as

$$K_a = [(\text{DMSO})_2]/[\text{DMSO}]^2 \quad (14)$$

Its temperature dependence (van't Hoff plot) gives the enthalpy of association ΔH as

$$\frac{d(\ln K_a)}{d(1/T)} = -\frac{\Delta H}{R} \quad (15)$$

In the calculations of the association constants (Table 4), the integrated intensities of respective components of the isotropic profiles of the ν_{10} line have been used. These have been considered proportional to the concentrations, and the latter have been found based on the temperature dependence of the DMSO density.[44,55] The values of K_a vary from 0.20 L mol^{-1} (23 °C) to 0.081 L mol^{-1} (100 °C). Their temperature dependence leads to ΔH = −11.7 ± 0.9 kJ mol^{-1} (Figure 5a).

As was noted in the Introduction, existing data on association constants significantly diverge, and our results at ambient temperature are closer to those found for acetonitrile solutions

dx.doi.org/10.1021/jp403858c | J. Phys. Chem. B 2013, 117, 9439−9448

Table 4. Intensities of the ν_{10} (A′) Line Corresponding to the C−S−C Vibrations of Free and Bonded DMSO Molecules, Concentrations of Monomeric and Dimeric DMSO Molecules, and Association Constants

temperature (°C)	I_{free} (arb. units)	I_{bond}[a] (arb. units)	c_{free} (mol L^{-1})	c_{bond}[a] (mol L^{-1})	K_a (L mol^{-1})
23	95 ± 15	90	4.8 ± 0.8	4.58	0.20 ± 0.04
30	99 ± 15	89	5.0 ± 0.8	4.47	0.18 ± 0.04
40	103 ± 12	86	5.2 ± 0.6	4.32	0.16 ± 0.03
50	107 ± 11	81	5.5 ± 0.5	4.11	0.14 ± 0.03
60	109 ± 10	68	6.0 ± 0.5	3.77	0.10 ± 0.02
70	116 ± 11	67	6.2 ± 0.6	3.60	0.09 ± 0.02
80	116 ± 10	66	6.2 ± 0.6	3.54	0.09 ± 0.02
90	116 ± 12	61	6.5 ± 0.6	3.38	0.08 ± 0.02
100	117 ± 12	60	6.4 ± 0.7	3.33	0.08 ± 0.02

[a]Less than 1% uncertainty.

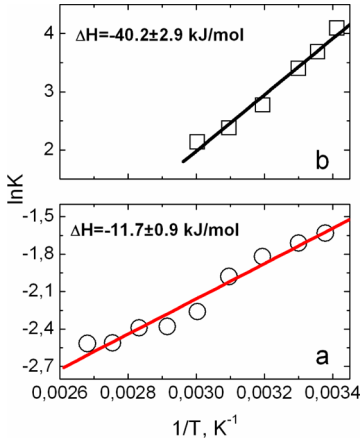

Figure 5. Van't Hoff plots for finding the enthalpy of association of DMSO. (a), our data; (b), data by Shikata and Sugimoto.[9]

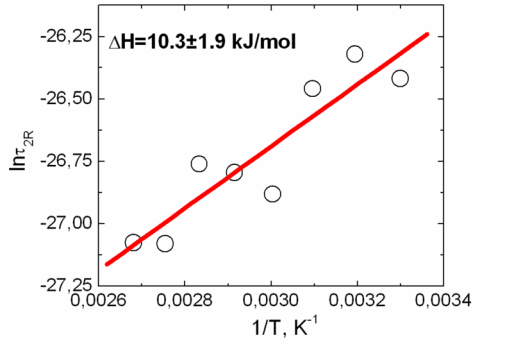

Figure 6. Temperature dependence of reorientation times of monomeric DMSO molecules.

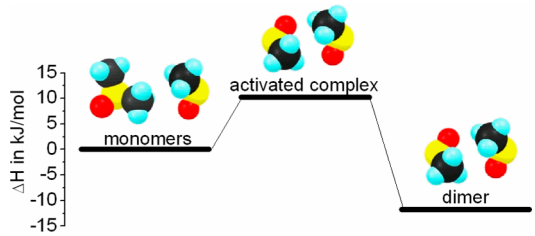

Figure 7. Energy levels of monomeric and dimeric DMSO molecules.

of DMSO, K_a = 0.22 L mol^{-1}.[7] We cannot explain why measurements of neat DMSO performed in our work and in refs 8 and 9 lead to different results. On the one hand, one may suggest that the choice of the ν_7 line for IR and Raman investigations in ref 8 has not been optimal. On the other hand, it seems that the values of K_a for concentrated solutions and neat DMSO in ref 8 (20−40 L mol^{-1}) and ref 9 (60 L mol^{-1}) are too high. Indirect evidence of this assumption gives our calculation of the enthalpy of association using the temperature dependence of K_a tabulated in ref 9; it leads to an abnormally high value, ΔH = −40 ± 3 kJ mol^{-1} (Figure 5b). Such a ΔH value is hardly acceptable, being characteristic of H-bonded systems (ΔH = −22−27 kJ mol^{-1} in neat liquid water[56]) instead of dipolar systems like DMSO.

Having the temperature dependence of the reorientation times of monomeric DMSO molecules (Table 1), one can estimate the potential barrier of reorientation as U = 10.3 ± 2.9 kJ mol^{-1} (Figure 6). Knowing this value, one can state that before trapping in a potential well, dimeric DMSO molecules have to pass an activation barrier requiring their proper alignment (Figure 7). The sum of this potential barrier and the absolute value of the enthalpy of association (22 ± 4 kJ mol^{-1}) well agrees with the potential barrier of collective rotations found in Rayleigh measurements (18.4 kJ mol^{-1}), which is considered to be characteristic of rotations of DMSO associates.[49]

CONCLUSIONS

Results presented in this paper enable us to suggest the following description of the molecular structure of liquid DMSO: The liquid consists of monomers and cyclic dimers, and the molar concentration of monomers varies from ∼5 M at 30 °C to ∼6.4 M at 100 °C. The C−S−C bonds are a sensitive indicator of the association process. In particular, the monomers and dimers demonstrate different frequencies of the C−S−C vibrations, ν_{10} (A′), and different hierarchies of respective characteristic times. In monomeric DMSO molecules, fast vibrational phase shifts are caused by fast, large amplitude torsional vibrations of attached methyl groups. On the contrary, vibrational modulation of dimeric molecules is slow, signifying that the DMSO molecules in dimers are rigidly connected together by dipolar forces (slow modulation limit). Reorientations of the monomeric DMSO molecules occur by elementary steps of 6−7° and follow the mechanism of free medium-angle diffusion. Reorientations of the dimeric molecules are slow and lie outside the time scale of Raman experiments.

dx.doi.org/10.1021/jp403858c | J. Phys. Chem. B 2013, 117, 9439−9448

On the other hand, in the region of the ν_3 (A′) vibration of C−H bonds, no splitting has been detected. This means that no signatures of hydrogen bonding between DMSO molecules exist, and in isotropic Raman, oscillators belonging to monomeric and dimeric molecules experience perturbations of very similar magnitude and have the same frequencies. Vibrational frequency modulation of C−H bonds follows customary collision concepts, and its characteristic time perfectly coincides with the time between collisions calculated in the framework of Enskog's model. In anisotropic Raman, rotational motions of monomeric and dimeric molecules take place with different speeds. However, because respective oscillators are indiscernible, rotational contributions from monomers and dimers in anisotropic Raman cannot be separated.

The association constants of the liquid DMSO vary from 0.20 L mol^{-1} (23 °C) to 0.081 L mol^{-1} (100 °C). Their temperature dependence gives the enthalpy of association of DMSO as $\Delta H = -11.7 \pm 0.9$ kJ mol^{-1}. Before trapping in this potential well, two monomeric DMSO molecules should be properly aligned, passing an activation barrier of 10.3 ± 2.9 kJ mol^{-1} determined in the analysis of the temperature dependence of reorientation times.

AUTHOR INFORMATION

Corresponding Author

*E-mail: kir@i.kiev.ua. Tel: +380-44-4243572. Fax: +380-44-4246240.

Notes

The authors declare no competing financial interest.

ACKNOWLEDGMENTS

S.A.K. gratefully acknowledges enlightening discussions and correspondence regarding molecular dynamics simulation of DMSO with Prof. Oleg N. Kalugin of Kharkov National University. The Raman experiments presented in this work have been carried out on the equipment of the Analytical Center of Common Access, Dagestan Scientific Center of the Russian Academy of Sciences, supported by the Russian Federation Basic Research Fund (Grant 13-03-00384A) and the Ministry of Education and Science of the Russian Federation (State Contract 16.552.11.7092).

REFERENCES

(1) Saytzeff, A. Über die Einwirkung von Saltpetersäure auf Schwefelmethyl und Schwefeläthyl. *Ann. Chem. Pharm.* **1867**, *144*, 145−148.
(2) Martin, D.; Weise, A.; Niclas, H.-J. The Solvent Dimethyl Sulfoxide. *Angew. Chem., Int. Ed.* **1967**, *6*, 318−334.
(3) Gores, H. J.; Barthel, J.; Zugmann, S.; et al. Liquid Nonaqueous Electrolytes. In *Handbook of Battery Materials*, 2nd ed.; Daniel, C., Besenhard, J. O., Eds.; Wiley-VCH: Weinheim, Germany, 2011; pp 525−626.
(4) Swanson, B. N. Medical Use of Dimethyl Sulfoxide (DMSO). *Rev. Clin. Basic Pharmacol.* **1985**, *5*, 1−33.
(5) Clark, T.; Murray, J. S.; Lane, P.; et al. Why are Dimethyl Sulfoxide and Dimethyl Sulfone Such Good Solvents? *J. Mol. Model.* **2008**, *14*, 689−697.
(6) Gajda, R.; Katrusiak, A. Electrostatic Matching versus Close-Packing Molecular Arrangement in Compressed Dimethyl Sulfoxide (DMSO) Polymorphs. *J. Phys. Chem. B* **2009**, *113*, 2436−2442.
(7) Figueroa, R. H.; Roig, E.; Szmant, H. H. Infrared Study on the Self-Association of Dimethyl Sulfoxide. *Spectrochim. Acta* **1966**, *22*, 587−592.
(8) Fawcett, W. R.; Kloss, A. A. Attenuated Total Reflection Fourier-Transform IR Spectroscopic Study of Dimethyl Sulfoxide Self-Association in Acetonitrile Solutions. *J. Chem. Soc., Faraday Trans.* **1996**, *92*, 3333−3337.
(9) Shikata, T.; Sugimoto, N. Dimeric Molecular Association of Dimethyl Sulfoxide in Solutions of Nonpolar Liquids. *J. Phys. Chem. A* **2012**, *116*, 990−999.
(10) Shikata, T.; Sugimoto, N. Reconsideration of the Anomalous Dielectric Behavior of Dimethyl Sulfoxide in the Pure Liquid State. *Phys. Chem. Chem. Phys.* **2011**, *13*, 16542−16547.
(11) Chalaris, M.; Marinakis, S.; Dellis, D. Temperature Effects on the Structure and Dynamics of Liquid Dimethyl Sulfoxide: A Molecular Dynamics Study. *Fluid Phase Equilib.* **2008**, *267*, 47−60.
(12) Adya, A. K.; Kalugin, O. N.; Volobuev, M. N.; et al. Microscopic Structure of Liquid Dimethyl Sulphoxide and Its Electrolyte Solutions: Molecular Dynamics Simulations. *Mol. Phys.* **2001**, *99*, 835−854.
(13) Onthong, U.; Megyes, T.; Bako, I.; et al. X-ray and Neutron Diffraction Studies and Molecular Dynamics Simulations of Liquid DMSO. *Phys. Chem. Chem. Phys.* **2004**, *6*, 2136−2144.
(14) Forel, M. T.; Tranquil, M. Spectres de Vibration du Diméthylsulfoxyde et du Diéthylsulfoxyde −d_6. *Spectrochim. Acta A* **1970**, *26*, 1023−1034.
(15) Skripkin, M. Yu.; Lindqvist-Reis, P.; Abbasi, A.; et al. Vibrational Spectroscopic Force Field Studies of Dimethyl Sulfoxide and Hexakis(dimethyl sulfoxide)scandium(III) Iodide, and Crystal and Solution Structure of the Hexakis(dimethyl sulfoxide)scandium(III) Ion. *Dalton Trans.* **2004**, *23*, 4038−4049.
(16) Perelygin, I. S.; Krauze, A. S.; Itkulov, I. G. Vibrational Data on the Effects of Self-Association on the Molecular Dynamics of Liquid Dimethyl Sulfoxide. *Zh. Prikl. Spektrosk.* **1990**, *52*, 414−419.
(17) Perelygin, I. S.; Itkulov, I. G.; Krauze, A. S. Molecular Association in Liquid Dimethyl Sulphoxide According to Raman Spectroscopy Data. *Russ. J. Phys. Chem.* **1991**, *65*, 1064−1068.
(18) Fini, G.; Mirone, P. Short-Range Orientation Effects in Dipolar Aprotic Liquids − III. Intermolecular Coupling of Vibrations in Sulfoxides, Sulfones, Nitriles and Other Compounds. *Spectrochim. Acta, Part A* **1976**, *32*, 625−629.
(19) Czeslik, C.; Kim, Y. J.; Jonas, J. Raman Frequency Non-coincidence Effect of Confined Liquid Dimethyl Sulfoxide. *J. Chem. Phys.* **1999**, *111*, 9739−9743.
(20) Paolantoni, M.; Gallina, M. E.; Sassi, P.; et al. Structural Properties of Glucose-Dimethylsulfoxide Solutions Probed by Raman Spectroscopy. *J. Chem. Phys.* **2009**, *130*, 164501−164509.
(21) Kirillov, S. A. Novel Approaches in Spectroscopy of Interparticle Interactions. Vibrational Line Profiles and Anomalous Non-Coincidence Effects. In *Novel Approaches to the Structure and Dynamics of Liquids: Experiments, Theories and Simulations*; Samios, J., Durov, V., Eds.; NATO ASI Series; Kluwer: Dordrecht, The Netherlands, 2004; pp 193−227.
(22) Lu, Z.; Manias, E.; Macdonald, D. D.; et al. Dielectric Relaxation in Dimethyl Sulfoxide/Water Mixtures Studied by Microwave Dielectric Relaxation Spectroscopy. *J. Phys. Chem. A* **2009**, *113*, 12207−12214.
(23) Bratu, I.; Klostermann, K.; Iliescu, T.; et al. Isotopic Substitution Effects on the Molecular Relaxation of Dimethylsulfoxide in Pure Liquid and Different Media. *J. Mol. Liq.* **1990**, *45*, 57−63.
(24) Iliescu, T.; Astilean, S.; Bratu, I. Raman Study of Vibrational Relaxation of Dimethylsulfoxide in Solutions. *J. Mol. Liq.* **1990**, *47*, 129−137.
(25) Rothschild, W. G. *Dynamics of Molecular Liquids*; Wiley: New York, 1984.
(26) Wang, C. H. *Spectroscopy of Condensed Media. Dynamics of Molecular Interactions*; Academic: Orlando, FL, 1985.
(27) Markarian, S. A.; Gabrielian, L. S.; Bonora, S. Vibrational Spectra of Dipropylsulfoxide. *Spectrochim. Acta, Part A* **2007**, *68*, 1296−1304.
(28) Luzar, A.; Soper, A. K.; Chandler, D. Combined Neutron Diffraction and Computer Simulation Study of Liquid Dimethyl Sulphoxide. *J. Chem. Phys.* **1993**, *99*, 6836−6848.

(29) Photiadis, G. M.; Papatheodorou, G. N. Vibrational Modes and Structure of Liquid and Gaseous Zirconium Tetrachloride and of Molten $ZrCl_4$−CsCl Mixtures. *J. Chem. Soc., Dalton Trans.* **1998**, 981−990.
(30) Kirillov, S. A.; Morresi, A.; Paolantoni, M.; et al. Possible Spectroscopic Manifestation of the Angular Group Induced Bond Alteration (AGIBA) Effect in Toluene. *J. Phys. Org. Chem.* **2007**, *20*, 568−573.
(31) Alía, J. M.; Edwards, H. G. M. Ion Solvation and Ion Association in Lithium Trifluoromethanesulfonate Solutions in Three Aprotic Solvents. An FT-Raman Spectroscopic Study. *Vib. Spectrosc.* **2000**, *24*, 185−200.
(32) Xuan, X.; Wang, J.; Zhao, Y.; et al. Experimental and Computational Studies on the Solvation of Lithium Tetrafluorobrate in Dimethyl Sulfoxide. *J. Raman Spectrosc.* **2007**, *38*, 865−872.
(33) Kubo, R. A. A Stochastic Theory of Line-Shape and Relaxation. In *Fluctuations, Relaxation and Resonance in Magnetic Systems*; ter Haar, G., Ed.; Scottish Universities' Summer School, 1961; Oliver and Boyd: Edinburgh, U.K., 1962; pp 23−68.
(34) Reid, G. D.; Wynne, K. Ultrafast Laser Technology and Spectroscopy. In *Encyclopedia of Analytical Chemistry*; Meyers, R. A., Ed.; Wiley: Chichester, U.K., 2000; pp 13644−13670.
(35) Cavalcante, A. O.; Ribeiro, M. C. C. Vibrational Dephasing of the Croconate Dianion in Different Environments. *J. Raman Spectrosc.* **2005**, *36*, 996−1000.
(36) Painter, P.; Sobkowiak, M.; Park, Y. Vibrational Relaxation in Atactic Polystyrene: An Infrared Spectroscopic Study. *Macromolecules* **2007**, *40*, 1730−1737, Vibrational Relaxation in Atactic Polystyrene: A Calculation of the Frequency Correlation Functions of Ring Stretching Modes and Their Variation with Temperature. 1738−1745.
(37) Painter, P.; Zhao, H.; Park, Y. Infrared Spectroscopic Study of Thermal Transitions in Poly(methyl methacrylate). *Vib. Spectrosc.* **2011**, *55*, 224−234.
(38) Kalampounias, A. G. Picosecond Dynamics From Lanthanide Chloride Melts. *J. Mol. Struct.* **2012**, *1030*, 125−130; Short-Time Vibrational Dynamics of Metaphosphate Glasses. *J. Phys. Chem. Solids* **2012**, *73*, 148−153.
(39) Kalampounias, A. G.; Tsilomelekis, G.; Bogosian, S. Short-Time Microscopic Dynamics of Aqueous Methanol Solutions. *Mol. Phys.* **2012**, *110*, 3095−3102.
(40) Kirillov, S. A. Time-Correlation Functions from Band-Shape Fits without Fourier Transform. *Chem. Phys. Lett.* **1999**, *303*, 37−42.
(41) Kirillov, S. A. Spectroscopy of Interparticle Interactions in Ionic and Molecular Liquids: Novel Approaches. *Pure Appl. Chem.* **2004**, *76*, 171−181.
(42) Einwohner, T.; Alder, B. J. Molecular Dynamics. VI. Free-Path Distributions and Collision Rates for Hard-Sphere and Square-Well Molecules. *J. Chem. Phys.* **1968**, *49*, 1458−1474.
(43) Dardi, P. S.; Cukier, R. I. Vibrational Relaxation in Fluids: A Critical Analysis of the Independent Binary Collision Theory. *J. Chem. Phys.* **1988**, *89*, 4145−4154; Can the Independent Binary Collision Theory Describe the Nonlinear Solvent Density Dependence of the Vibrational Energy Relaxation Rate? **1991**, *95*, 98−102.
(44) Oswal, S. L.; Patel, N. B. Speeds of Sound, Isentropic Compressibilities, and Excess Volumes of Binary Mixtures of Acrylonitrile with Organic Solvents. *J. Chem. Eng. Data* **2000**, *45*, 225−230.
(45) Kirillov, S. A.; Pavlatou, E. A.; Papatheodorou, G. N. Instantaneous Collision Complexes in Molten Alkali Halides: Picosecond Dynamics from Low-Frequency Raman Data. *J. Chem. Phys.* **2002**, *116*, 9341−9352.
(46) Kirillov, S. A. Interactions and Picosecond Dynamics in Molten Salts: A Review With Comparison to Molecular Liquids. *J. Mol. Liq.* **1998**, *76*, 35−95.
(47) Kirillov, S. A.; Yannopoulos, S. N. Vibrational Dynamics as an Indicator of Short-Time Interactions in Glass-Forming Liquids and Their Possible Relation to Cooperativity. *J. Chem. Phys.* **2002**, *117*, 1220−1230.
(48) Clever, H. L.; Westrum, E. F. Dimethyl Sulfoxide and Dimethyl Sulfone. Heat Capacities, Enthalpies of Fusion, and Thermodynamic Properties. *J. Phys. Chem.* **1970**, *74*, 1309−1317.
(49) Higashigaki, Y.; Christensen, D.; Wang, C. H. Studies of the Reorientational Motion and Intermolecular Interaction of Dimethyl Sulfoxide in Water by Depolarized Rayleigh Scattering. *J. Phys. Chem.* **1981**, *85*, 2531−2535.
(50) Gordon, R. G. Correlation Functions for Molecular Motion. *Adv. Magn. Reson.* **1968**, *3*, 1−42.
(51) Nafie, L.; Peticolas, W. Reorientation and Vibrational Relaxation as Line Broadening Factors in Vibrational Spectroscopy. *J. Chem. Phys.* **1972**, *57*, 3145−3156.
(52) Ivanov, E. N.; Valiev, K. A. Rotational Brownian Motion. *Usp. Fiz. Nauk* **1973**, *109*, 31−47.
(53) Gordon, R. G. Molecular Motion and the Moment Analysis of Molecular Spectra in Condensed Phases. I. Dipole-Allowed Spectra. *J. Chem. Phys.* **1963**, *39*, 2788−2798; Molecular Motion and the Moment Analysis of Molecular Spectra. II. The Rotational Raman Effect. **1964**, *40*, 1973−1986; Molecular Motion and the Moment Analysis of Molecular Spectra. III. Infrared Spectra. **1964**, *41*, 1819−1830; Molecular Motion in Infrared and Raman Spectra. **1965**, *43*, 1307−1313.
(54) Bartoli, F. J.; Litovitz, T. A. Analysis of Orientational Broadening of Raman Line Shapes. *J. Chem. Phys.* **1972**, *56*, 404−413, Raman Scattering: Orientational Motions in Liquids. 413−426.
(55) Karapetyan, Yu. A.; Eychis, V. N. *Physicochemical Properties of Non-Aqueous Electrolyte Solutions* (In Russian); Khimiya: Moscow, 1989.
(56) Walrafen, G. E.; Fisher, M. R.; Hokmabadi, M. S.; et al. Temperature Dependence of the Low- and High-Frequency Raman Scattering from Liquid Water. *J. Chem. Phys.* **1986**, *85*, 6970−6983.